

01 Jan 1961

Effects of Calcining Temperature on the Physical Properties of Zirconate Ceramics

P. D. Ownby

Missouri University of Science and Technology, ownby@mst.edu

Follow this and additional works at: https://scholarsmine.mst.edu/matsci_eng_facwork



Part of the [Materials Science and Engineering Commons](#)

Recommended Citation

P. D. Ownby, "Effects of Calcining Temperature on the Physical Properties of Zirconate Ceramics," University of Utah, Jan 1961.

This Book is brought to you for free and open access by Scholars' Mine. It has been accepted for inclusion in Materials Science and Engineering Faculty Research & Creative Works by an authorized administrator of Scholars' Mine. This work is protected by U. S. Copyright Law. Unauthorized use including reproduction for redistribution requires the permission of the copyright holder. For more information, please contact scholarsmine@mst.edu.

EFFECTS OF CALCINING TEMPERATURE ON THE
PHYSICAL PROPERTIES OF ZIRCONATE CERAMICS

by

P. Darrell Ownby

A thesis submitted to the faculty of the
University of Utah in partial fulfillment
of the requirements for the degree of

Bachelor of Science
Department of Ceramic Engineering

University of Utah

June, 1961

Approved Ivan B. Lutter
Department Head

ACKNOWLEDGEMENT

The author wishes to express sincere appreciation to the following people for their assistance and guidance:

Dr. Ivan B. Cutler, Professor and Department Head
of Ceramic Engineering, University of Utah

Dr. Milton E. Wadsworth, Professor and Department
Head of Metallurgical Engineering, University of Utah

Mr. Theron M. Lambert, Director of Research,
Electro Ceramics

Dr. Edmond P. Hyatt, Production Manager, Electro
Ceramics

Mr. Kent Peterson, Electro Ceramics

The author also wishes to acknowledge the assistance of
Electro Ceramics, Inc., who sponsored the project.

EFFECTS OF CALCINING TEMPERATURE ON THE
PHYSICAL PROPERTIES OF ZIRCONATE CERAMICS

Introduction:

1. Other calcining problems.

Many observers have found that the chemical and physical properties of metal oxide ceramics vary with the method with which the oxides are prepared prior to sintering.

Quirk¹¹, in his studies on the sinterability of oxide powders BeO and MgO, found of particular interest the great influence of the calcining treatments on the sinterability of the active oxide powders. He, along with many independent observers, found that certain oxides are especially reactive and readily sinterable when they are prepared by carefully controlled pyrolysis of the starting compounds. In particular, he stated that the temperature of pyrolysis or calcining can have a marked effect on the sintering of berillia and magnesia powders. He reported that powders calcined at an optimum calcining temperature produced sintered pieces which more nearly approached the theoretical density.

Iida and Ozaki³ observed the same phenomenon in their study on the sintering of high-purity nickel-oxide, defining an even more specific optimum calcining temperature in relation to the final bulk densities of the fired pieces. These Japanese researchers also found that the particle size of the calcined powder increased with the increased calcining temperature.

Quirk, Mosley, and Duckworth¹⁰, in studying the sinterability of BeO noted the critical effects of the calcining temperature on sintering. They reported a calcination temperature where maximum density occurs at varied firing temperatures. They discovered that at a point above this

temperature the density began dropping in the sintered pieces because the powders were essentially "dead burned." By the use of X-Ray diffraction, the calcined powders were examined and found to have a change in lattice parameters with calcination temperature. They suggest that this is due to a relief in strain of the crystals caused, possibly, by impurity ejection. The indices of refraction were also measured as a function of calcining temperature with a petrographic microscope and found to increase with temperature.

2. The critical variables of the calcining process

- | | |
|--|---|
| a. The calcining temperature | e. The form of the starting materials: |
| b. The length of soaking time | Chemical form |
| c. The rate of temperature increase
and decrease | Crystalline form |
| d. The particle size:
of raw materials
of calcined materials | f. The impurities;
in raw materials
introduced by apparatus |
| | g. The preparation techniques |
| | h. The atmosphere |

In this study, all variables were held constant except calcining temperature.

3. Calcining to form lead-zirconate-titanate.

The problem of calcining the lead-zirconate-titanate materials is quite different from any of the above mentioned studies. It involves not just a decomposition reaction, e.g., as in the case of $\text{Be}(\text{OH})_2 \rightarrow \text{BeO} + \text{H}_2\text{O}$ or the formation of metallic oxides by decomposition of their nitrates, sulphates, oxalates, or carbonates, but also a complicated formation reaction. Starting with the raw materials PbO , TiO_2 , and ZrO_2 , a solid solution between PbTiO_3 and PbZrO_2 must be formed to get the desired $\text{Pb}(\text{ZrTi})\text{O}_3$. Due to the additional complications and variables involved in calcining the desirable

zirconate ceramics, many different and conflicting methods have been reported in the production process. One of the most important variables in calcining the zirconate is the calcining temperature. B. Jaffe, Roth, and Marzullo⁴, in one of the first papers on the subject, report a suitable calcining temperature of 1472° F., and three years later, Okazaki⁹ reported the same temperature. More recently, Kulcsar⁷ reported a successful calcining temperature of 1530° to 1560° F.

Jaffe, Roth, and Marzullo⁴ studied the solid solution series PbZrO_3 - PbTiO_3 near the morphotropic transformation boundary between the tetragonal and rhombohedral solid solution phases. They explained that the morphotropic transformations occur as the composition of a solid solution system is varied because of free energy differences between two or more alternate crystallographic modifications of a given basic structure type. As one ion replaces another in a solid solution, the energies of the different structures change and the crystal assumes the structure having the minimum free energy. In the PbZrO_3 - PbTiO_3 it was found that the c/a ratio of the tetragonal PbTiO_3 was decreased as the PbZrO_3 was added in solid solution until a morphotropic phase boundary occurred at 55 mole % PbZrO_3 . Compositions higher in PbZrO_3 content were rhombohedral. In the proximity of the compositional morphotropic transformation, the room temperature dielectric constant and the induced piezoelectric effects of the ceramic were enhanced. The results of most of the other investigators support this fact. The composition $\text{Pb}(\text{Ti}_{.46}\text{Zr}_{.54})\text{O}_3$ was used throughout this investigation. This composition is expected to be predominantly tetragonal with a minor content of the rhombohedral phase.

The method used by Roth, Jaffe, and Marzullo to prepare, calcine, and fire the lead-zirconate-titanate ceramics seemed to be accepted by previous authors and generally followed by subsequent authors. The raw

materials used were a commercially-pure grade of ZrO_2 and TiO_2 and a reagent grade of PbO . These materials, in pressed pellet form, were calcined at $1472^\circ F.$ for one-half hour in a covered platinum crucible. Organic binders were avoided by these investigators.

Roberts⁴ pointed out that lead oxide in lead zirconate and its solid solutions is volatile. Cognizant of the advice of Roberts, Roth and associates used special controls to prevent PbO loss. They placed the specimens in a large platinum crucible separated from one another by platinum foil (Fig. 2). A pellet of $PbO + ZrO_2$ enriched in PbO over the 1:1 molar ratio by 4 weight percent, was placed on top of the stacked specimens. This pellet provided an atmosphere enriched in PbO vapor to retard evaporation of lead-zirconate-titanate from the specimens. A smaller crucible was inverted over the stack of specimens and another atmosphere pellet was placed on top of it. The larger outer crucible was also covered. They found it possible, by varying the weights of their atmosphere pellets, to cause the specimens to lose weight, remain unchanged, or gain weight.

Experimental Procedure:

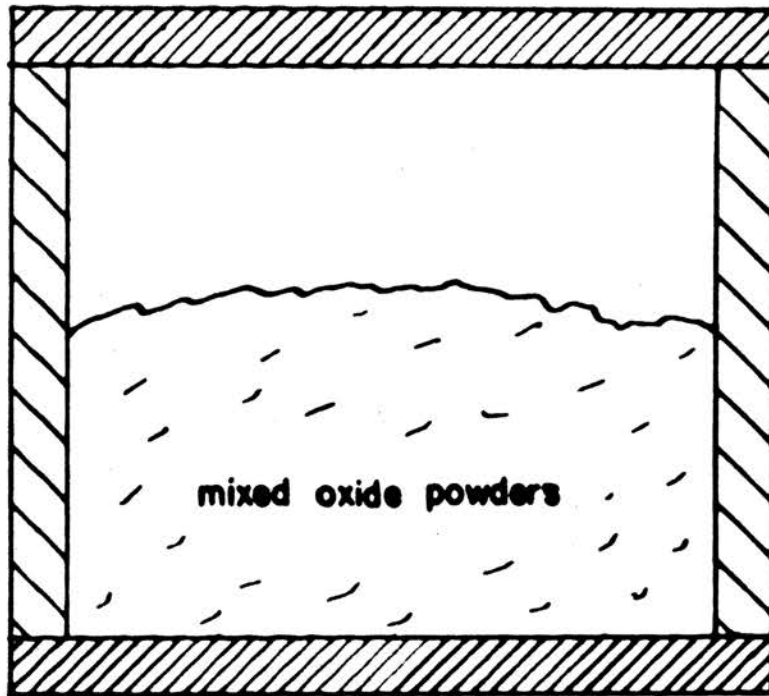
The materials used in this investigation included commercially-pure grades of oxides of lead, titanium, and zirconium. Chemically pure niobium oxide was used. Each of these raw materials was tested for average particle size on a Fisher sub-sieve sizer. 2000 gm batches were weighed out, which were calculated to yield the composition $Pb(Zr_{.54}Ti_{.46})O_3$ plus 1 per-cent niobium when calcined in a controlled lead atmosphere. Each batch was wet ball-milled for one hour for intimate mixing using de-ionized water. The slurries were dried under infrared lamps and the dried material was broken up with a mortar and pestle. $BaTiO_3$ crucibles were prepared by lapping the end of a hollow $BaTiO_3$ cylinder 4 inches in diameter and 3 inches long. $BaTiO_3$ discs, 4 inches in diameter were lapped smooth and used as bottoms and lids, (Fig. 1). This provided tightly sealed containers for calcining and firing the lead-zirconate-titanate ceramics. 500 gms of the mixed powder was put in each crucible and calcined by heating at a rate of $150^\circ F/hour$ and soaking for three hours in a Harper electric kiln. Samples were tested at ten different calcining temperatures, ranging between $1450^\circ F$ and $2000^\circ F$.

After calcining, the powder was broken up and ball-milled wet with de-ionized water for three hours. The slurries were again dried under infrared lamps. The average particle size was then determined with the Fisher sub-sieve sizer. Samples of the calcined powder and the raw material powders were taken for X-Ray diffraction tests and electron micrographs. X-Ray diffraction patterns were obtained using a Norelco Gieger-counter type X-Ray diffractometer, using CuK_{α} radiation. The tests were made on powder samples dried from a slurry onto a glass slide. An attempt was made on one series of tests to standardize the intensity of the peaks by adding 10% NaCl to the powder and mixing it in petroleum jelly. The expected uniform

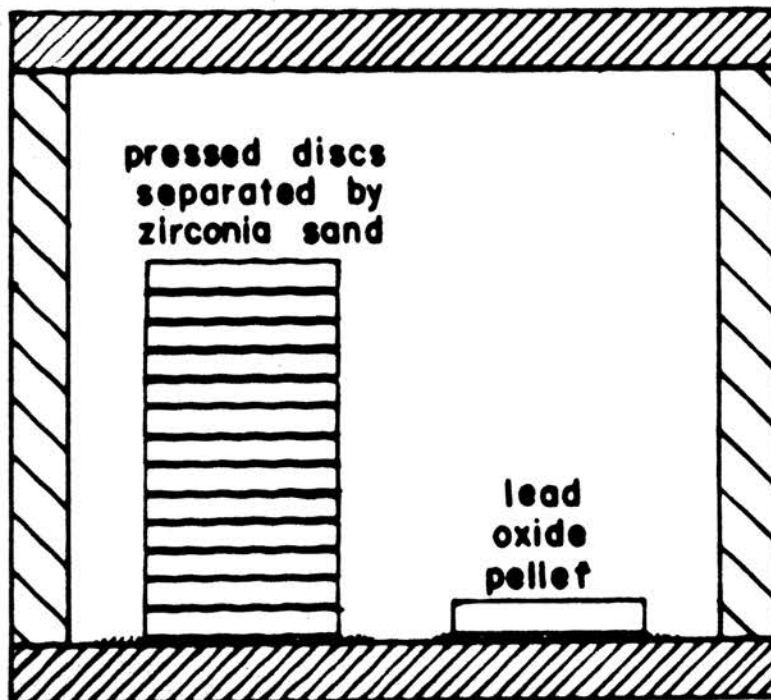
salt peaks were not obtained, however, the intensity of the lead-zirconate-titanate peaks showed the same results as other samples not "salted". Since all of the calcined material (regardless of calcining temperature) passed through a 325 mesh screen, the screened powders were examined under the electron microscope. Micrographs were taken to compare particle size as a check on the Fisher sub-sieve sizer tests. The micrographs confirmed the results of the Fisher sub-sieve sizer and further revealed that the larger "particles" at all calcining temperatures were glomerates made up of small particles (Fig. 3). A suspension of polyvinyl alcohol in water was added as a binder and calcium stearate as a lubricant to aid the pressing operation. The powder was pressed into discs 1.125 inches in diameter and .1 inch thick. The discs were dried and sintered in the closed BaTiO₃ crucibles at temperature and time conditions which produced maximum fired density. Fine zirconia sand was used between the discs and an 8 gm pressed lead oxide pellet was placed inside each crucible to provide a lead atmosphere to prevent lead loss during firing.

After cooling, densities were determined for each piece by the water displacement method. ($\rho = \frac{\text{dry weight}}{\text{dry wt.} - \text{submerged wt.}}$). The discs were lapped smooth to $.080 \pm .003$ inches. A silver paste (Dupont conductive silver #7095) was applied to the discs by silk screen and then fired on to form electrodes. The discs were poled in 100°C silicon dielectric oil at 100 kv/mil for 15 minutes. Twenty-four hours after poling, the capacitance, dissipation, resonant frequency, resonant voltage, anti-resonant frequency, and anti-resonant voltage were measured. From these observations, the dielectric constant, planar coupling coefficient and frequency constants were calculated.

BaTiO₃ CRUCIBLES



For Calcining

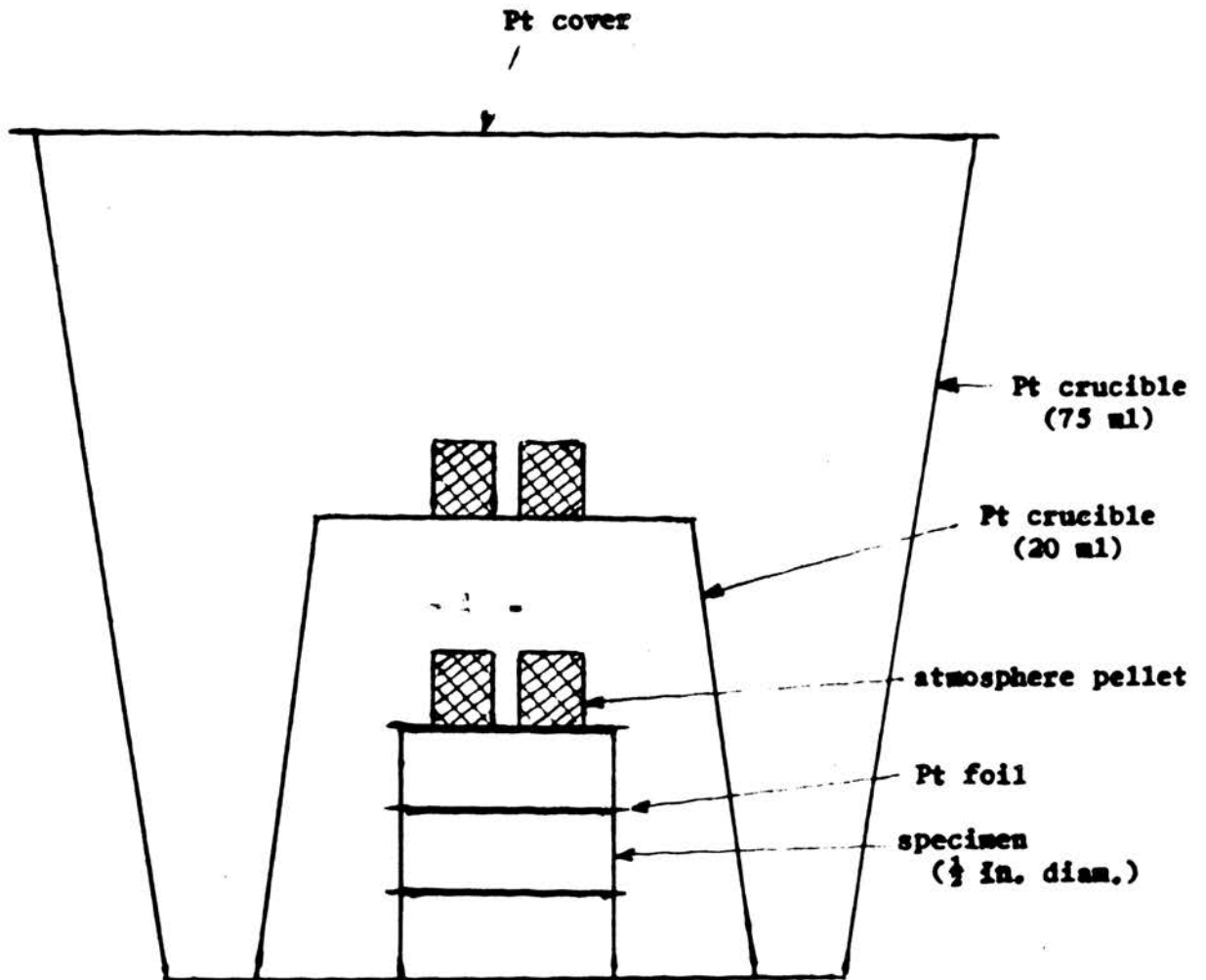


For Sintering

FIG. 1

DATA

<u>Calcining Temperature</u>	<u>Density</u>	<u>Dielectric Constant</u>	<u>Dissipation</u>	<u>Planar Coupling Coefficient</u>	<u>Frequency Constant</u>
1450	7.35	1062		.320	59.2
1550	7.31	1200	.75	.455	84.2
1650	7.43	1200	1.50	.520	81.2
1700	7.57	1700	1.52	.615	80.0
1750	7.41	1329	1.50	.584	81.1
1800	7.38	1383	1.02	.521	83.1
2000	7.17	1222	1.44	.447	109.1



Platinum Crucible used to fire Zirconate Ceramics
(Cross-hatched rectangles represent $\text{PbO}\cdot\text{ZrO}_2$ pellets slightly enriched in PbO .)

FIG. 2

Calcine Temperature vs Particle Size

Average
Particle
Size
(μ)

34

32

30

28

1650

1700

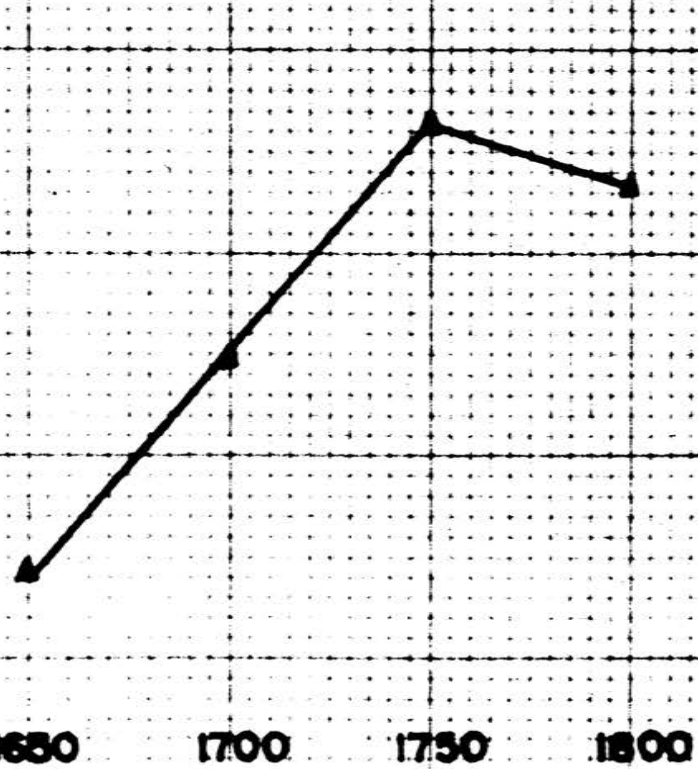
1750

1800

Calcine Temperature $^{\circ}$ F

FIG. 3

- 10 -



Calcine Temperature vs Density

Density

7.6

7.4

7.2

7.0

1400

1500

1600

1700

1800

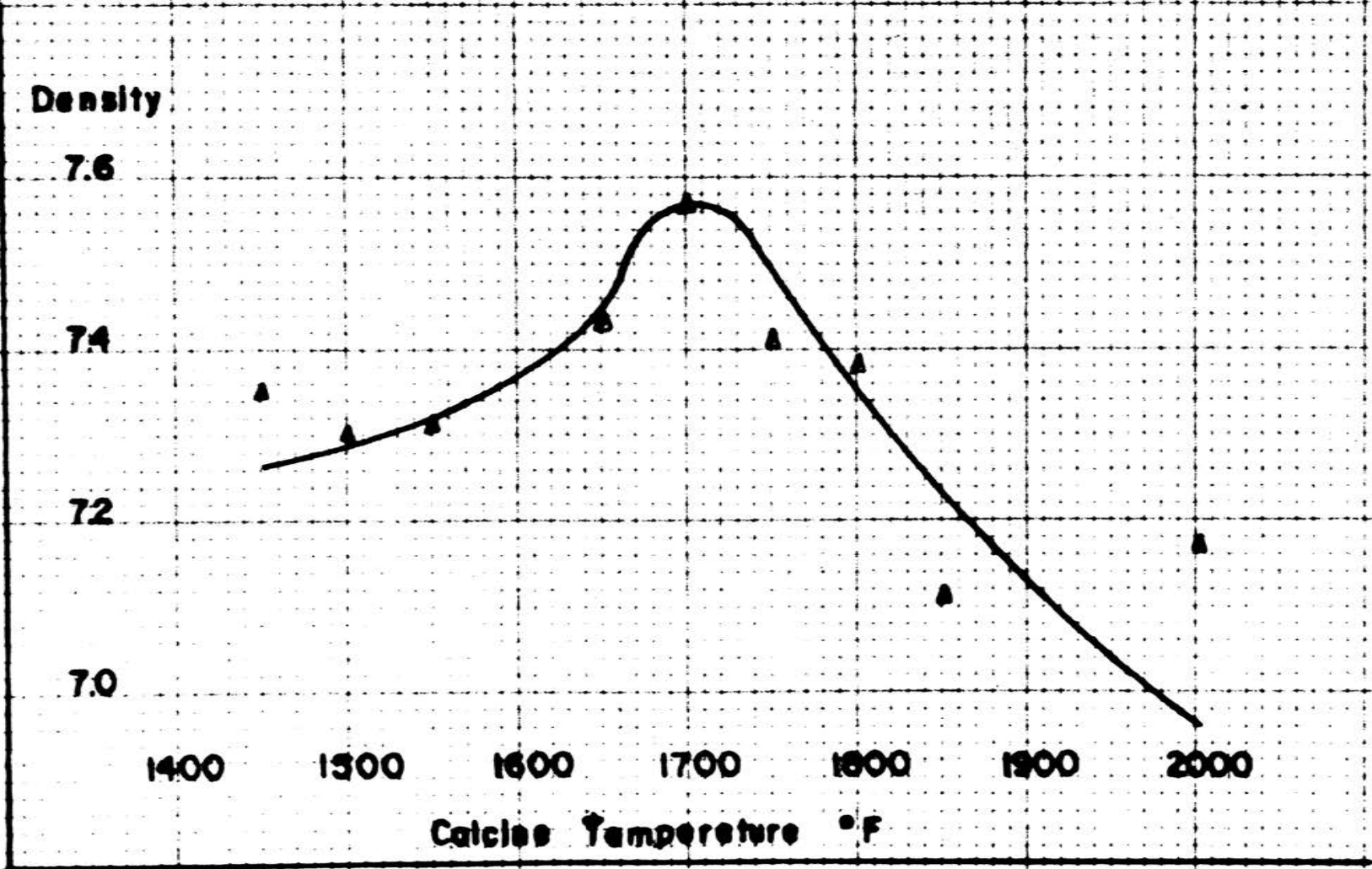
1900

2000

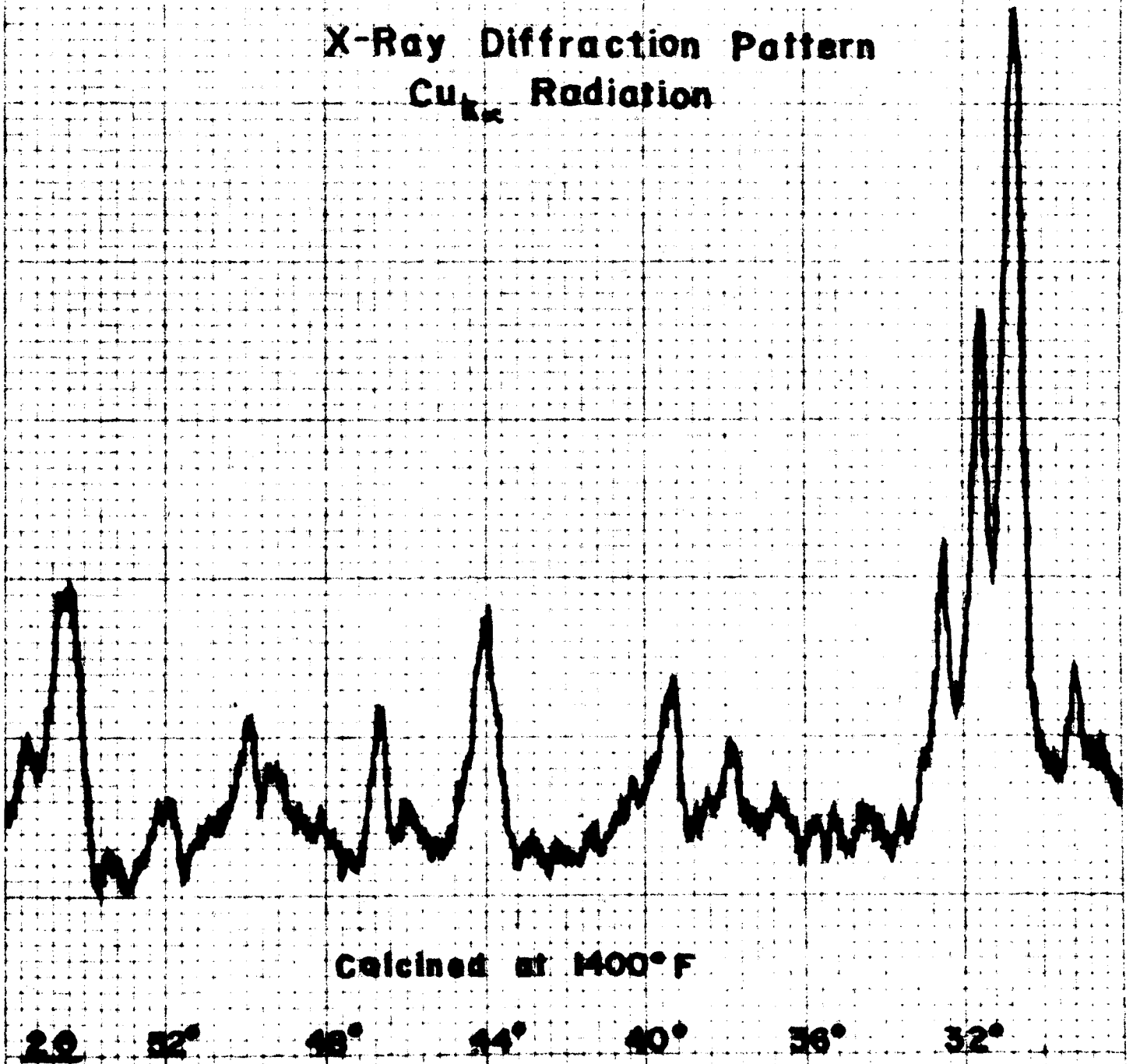
Calcine Temperature °F

FIG. 4

11



X-Ray Diffraction Pattern Cu_{K α} Radiation



Calcined at 1400°F

FIG. 3

X-Ray Diffraction Pattern

Cu_{K α} Radiation

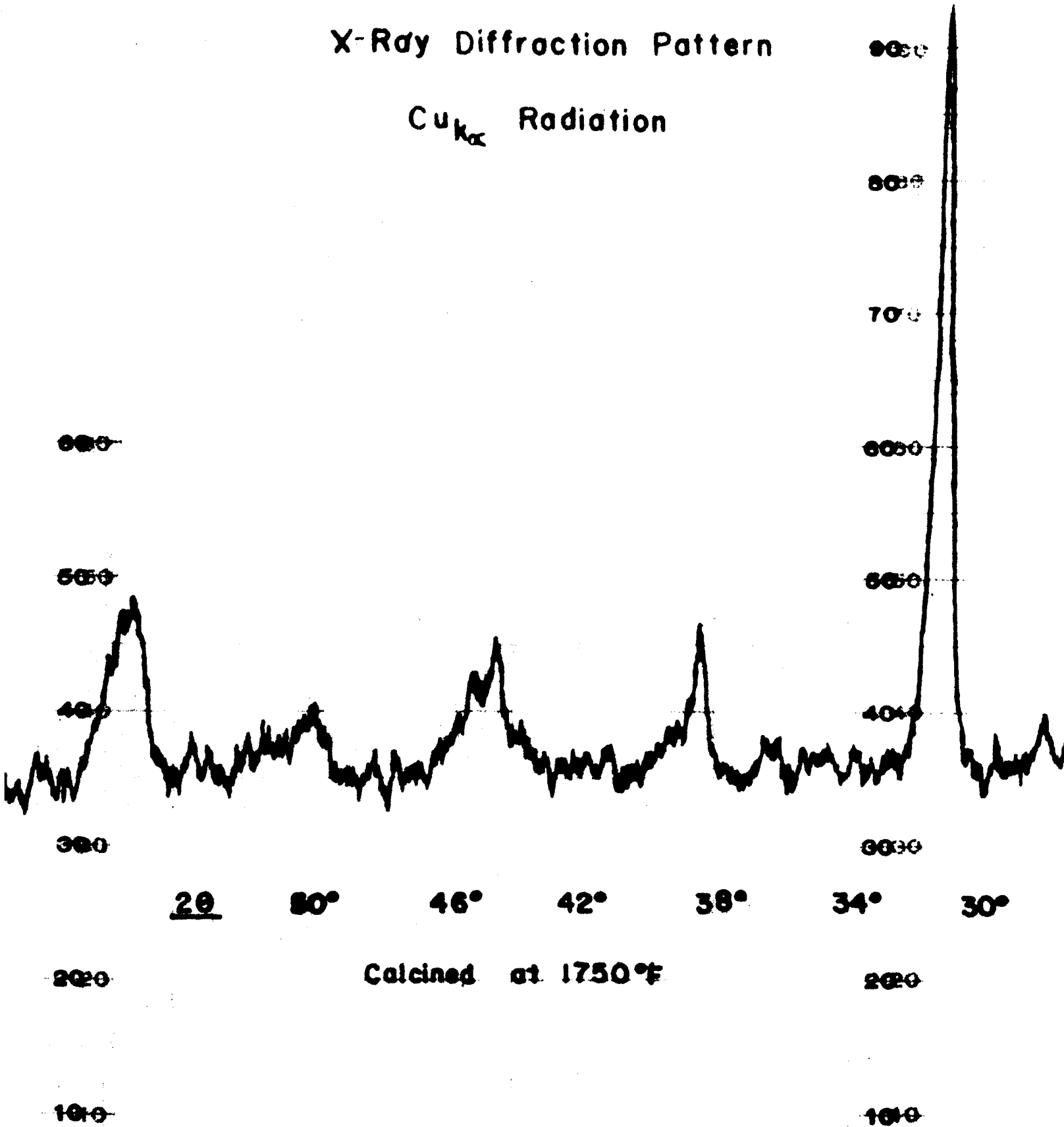
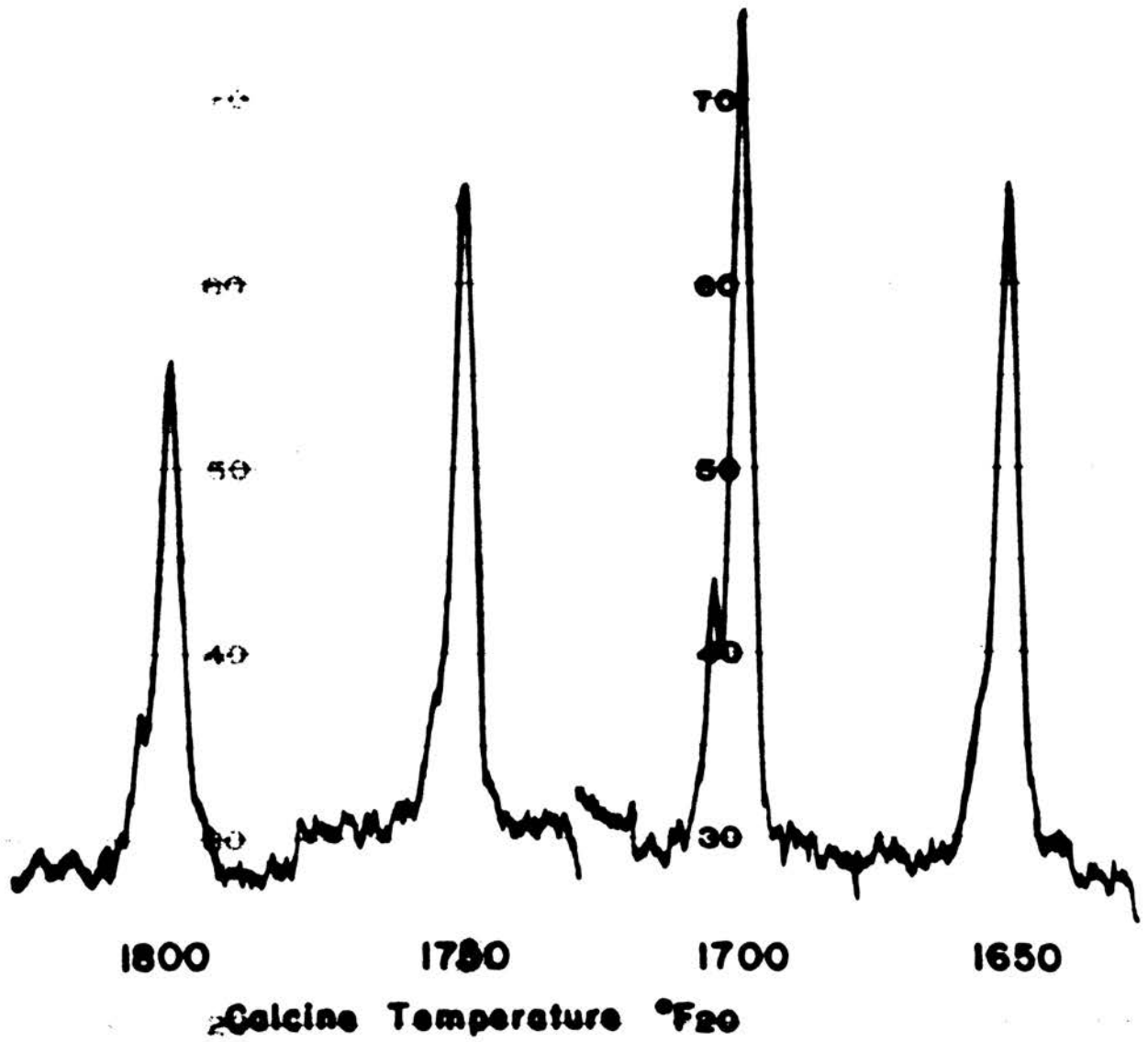


FIG. 6

X-Ray Diffraction Patterns
most intense peak only $2\theta = 31^\circ$
 $^{60}\text{Co}_{K\alpha}$ radiation



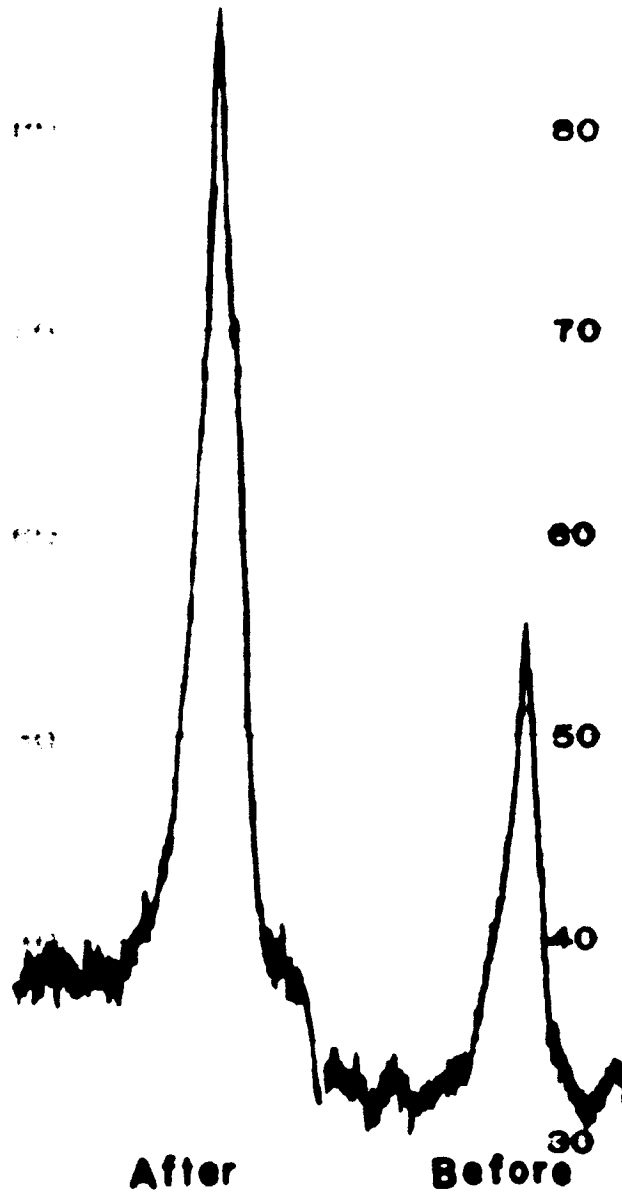
These peaks show relative intensity on this Fig. only and the intensity cannot be compared to Figs. 5, 6, and 8. as the diffraction recorder settings were decreased for this Figure.

FIG. 7

X-Ray Diffraction Patterns

most intense peak only

$\text{Cu}_{k\alpha}$ radiation



annealed at 1800°F

FIG. 8

Calcine Temperature vs Dielectric Constant

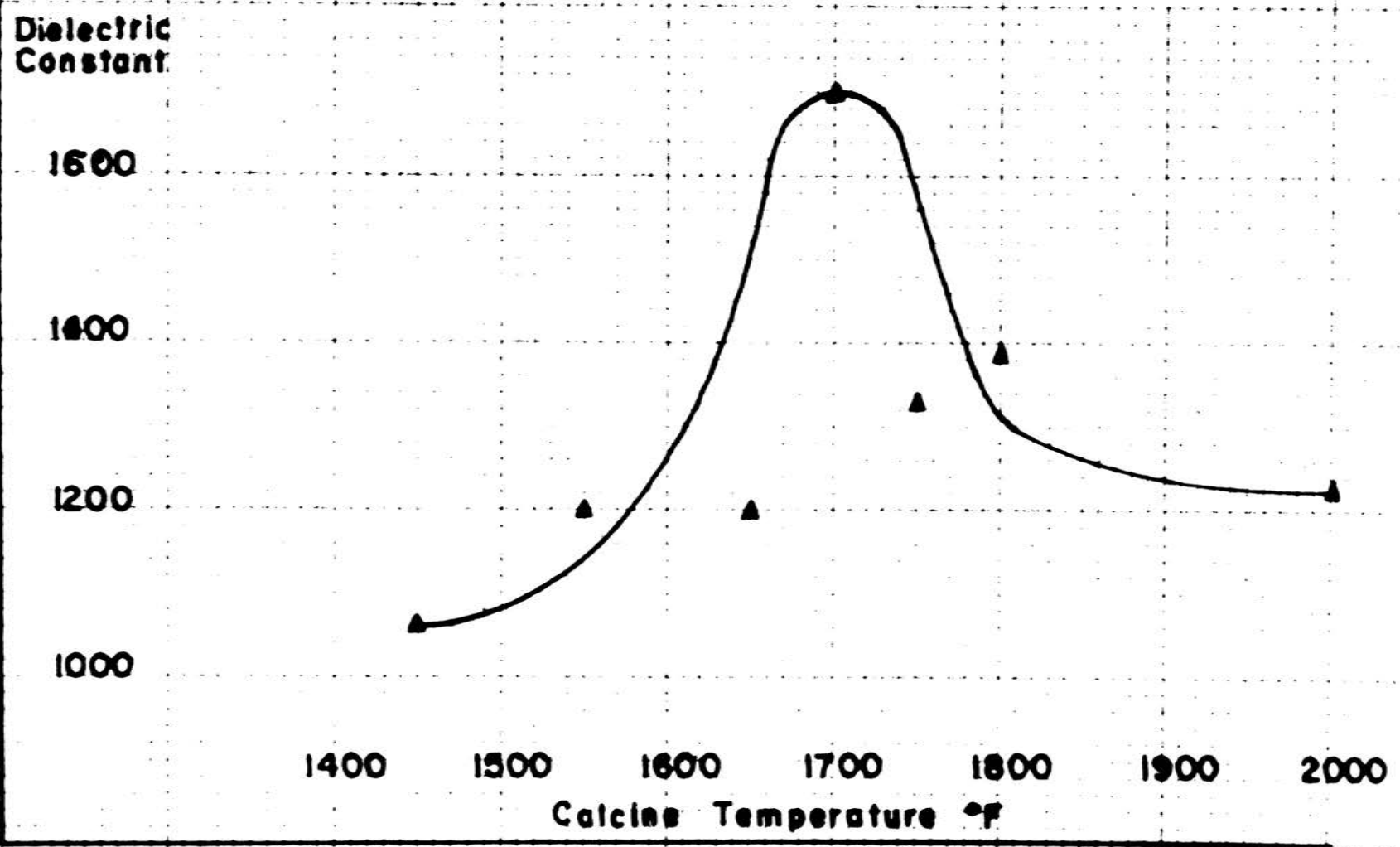


FIG. 9

Calcine Temperature vs Frequency Constant

Frequency
Constant
(kc/in)

100

90

80

70

1400

1500

1600

1700

1800

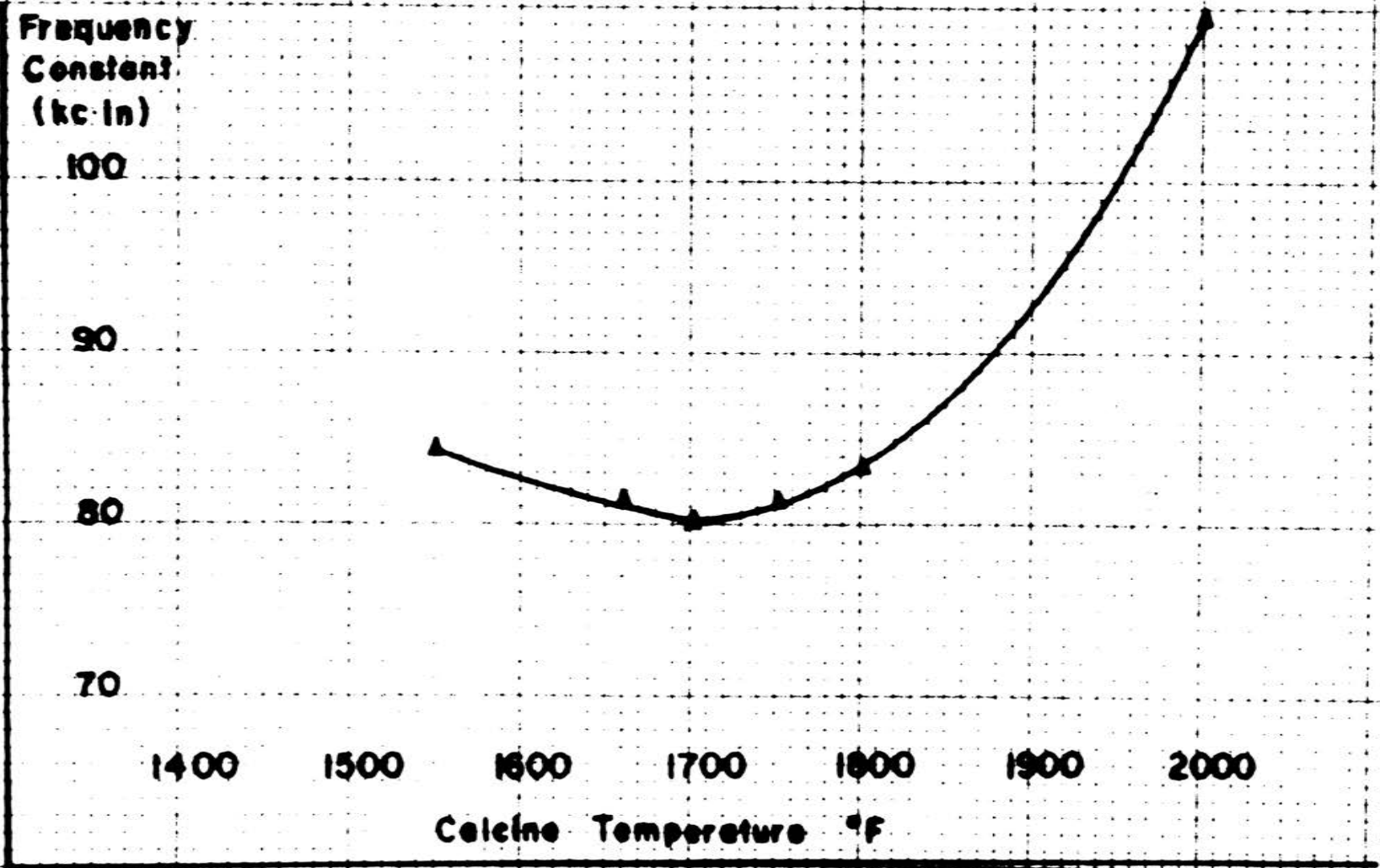
1900

2000

Calcine Temperature °F

FIG. 10

17



Calcine Temperature vs Coupling Coefficient

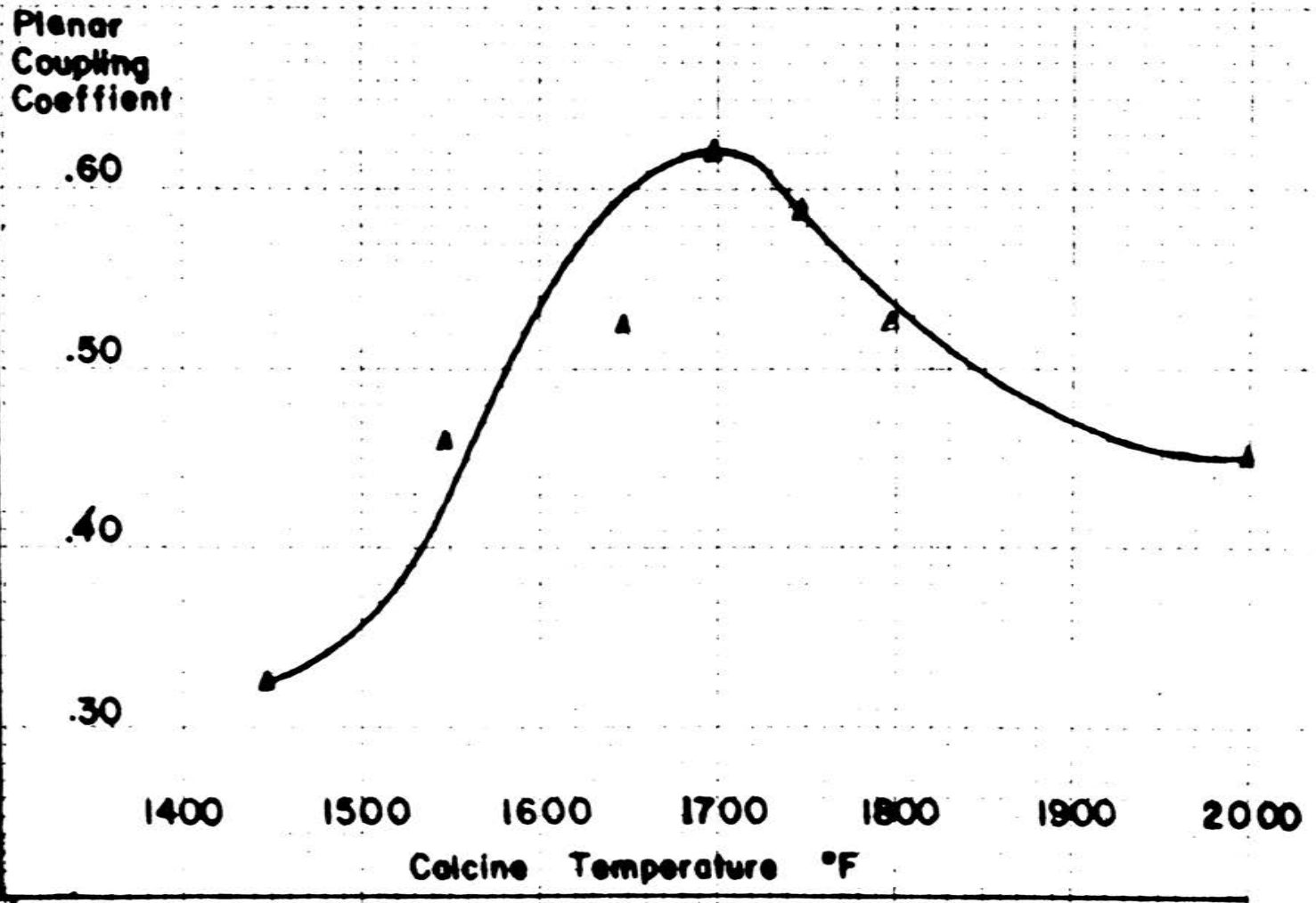


FIG. 1

Discussion of Results:

It can be seen from the data table and the graphical representations of the physical constants as functions of calcining temperature, that there is an optimum lead-zirconate-titanate calcining temperature as expected. Fig. 4 (Density vs. Calcining Temperature) shows that the density increases at an increasing rate to a maximum at 1700° F. This phenomenon is easily understood when the reaction taking place is considered. At a temperature below those used for calcining, the lead combines with the oxides of zirconium and titanium to form $PbZrO_3$ and $PbTiO_3$, respectively. These two compounds were detected by X-Ray diffraction methods at 1400°F., (Fig. 5). The most intense peak (shown here at 30.7°) represents the maximum $PbZrO_3$ peak with a "d spacing" of 2.94. The peaks at 44° and 54.4° also represent $PbZrO_3$. $PbTiO_3$ is represented by the peaks at 31.5°, 39.3°, and 46.7° and 55.3°. The remaining peaks at 29.2°, 32.5°, and 37.8° represent PbO . The free titanium and zirconium oxides do not show up well on the pattern because of the high absorption of the Pb^{++} ion. Subsequent X-Ray tests showed that as the calcining temperature is increased, the PbO peaks diminish and vanish. The $PbZrO_3$ and $PbTiO_3$ peaks grow until they merge into single, sharp peaks with different 2θ angles and consequent d-spacings than either the zirconate or the titanate, (Fig. 6 and Fig. 7), (lead-zirconate-titanate peaks @ 1650°, 1700°, 1750°, 1800°). These values are indicative of the solid solution. It can be seen that the density increases as the oxides of lead, zirconium, and titanium combine to form the more dense compounds $PbTiO_3$ and $PbZrO_3$. Further, as the temperature increases above 1400°F, not only is more zirconate and titanate formed from the original oxides but the zirconate and titanate themselves combine to form a solid solution.

There is also another mechanism which this author proposes as an answer to the density increase, the optimization of the density curve, and the density decrease above optimum temperature. It can be explained by looking at the calcine temperature vs. powder particle size curve as measured by the Fisher sub-sieve sizer, (Fig. 3). This instrument measures the ease with which air will pass through a powder compact and therefore it indicates the glomerate size and not particle size in the strict sense. As the calcine temperature was increased and the sintering process started, the particles started sticking together as glomerates containing voids. After calcining, when these glomerates were pressed into pieces, the green density was an inverse function of the amount of voids. As the calcining temperature approached the optimum (1700°F), the voids reached a minimum as sintering increased. Beyond this temperature, the larger particles formed by sintering appear to have yielded a powder, which when pressed, formed an increasingly less dense piece. This phenomenon can be observed on Fig. 8, where powder calcined at 1800° was examined by X-Ray diffraction before and after ball-milling. A great difference in intensity of the most prominent peak ($2\theta=31^\circ$) can be seen. Therefore, it is theorized that the green density of the pieces, as a function of the calcination temperature, was an embryonic preview of the fired densities. In other words, the more dense pre-fired piece would probably produce the more dense fired piece.

It is the opinion of this author that the same phenomenon which produced the final density vs. calcine temperature curve was one of the many factors which caused both the electrical properties to optimize and the diffraction peaks to maximize in direct relationship to it. As the density increases, the "free" dielectric constant, the one which was measured at low frequency, also increases, (Fig. 9). Mathematically, $\epsilon^T = \frac{(\text{const.}) (C_p) (\text{thickness})}{(\text{Area})}$ where C_p is the capacitance.

Therefore,

$$\epsilon^T \propto \frac{t}{d^2}$$

$$\epsilon^T \propto \rho$$

The frequency constant N , on Fig. 10, is seen to reach a minimum at the temperature where the density is a maximum.

$$N = F_r d$$

where F_r is the resonant frequency

$$F_r = \frac{v}{\lambda} \text{ where } v \text{ is the velocity of sound in the medium}$$

λ is the wavelength

$$v \propto \sqrt{\frac{E'}{\rho}} \text{ where } E' \text{ is the effective Young's Modulus}$$

$$N \propto \sqrt{\frac{E'}{\rho}}$$

Therefore, within the limits of this discussion, the frequency constant and the planar coupling coefficient seem to be functions of the density.

The planar coupling coefficient (Fig. 11) is a function of the remnant polarization of the ceramic piece, the piezoelectric constant which relates mechanical strain to electric field, the effective Young's Modulus, and the free dielectric constant. Although it is difficult to pinpoint the exact causes of the observed phenomenon, the following suggestions are submitted as possibilities for further research in order to more fully understand the mechanisms of this familiar optimization phenomenon.

Low density is usually due to pores in the ceramic material. These pores may act as domain growth hindering impurities. The polarization of the ceramic pieces is a function of the domain growth and the planar coupling coefficient is in turn a function of the polarization.

Conclusions:

There is a calcining temperature at which lead-zirconate-titanate ceramics produced thereby yield optimum physical and electrical properties.

This temperature is higher than reported by previous authors because the method of controlling atmosphere conditions was superior, indicated by the values of the physical constants being more desirable than any yet published.

Closed titanate crucibles can be used satisfactorily as a means to carefully control atmosphere conditions.

Many physical properties of electrical ceramic bodies may be functions of the density of the piece.

BIBLIOGRAPHY

1. Berlincourt, D., Jaffe, B., and Krueger, H.A., "Transducer Properties of Lead-Titanate-Zirconate Ceramics", IRE Transactions of Ultrasonic Engineering, Vol. UE 7, February 1960, #1.
2. Gulton, Leslie K., "Ceramic Transducers - ZrO_2 , TiO_2 , PbO ," U.S. 2,892,955, June 30, 1959, (13).
3. Iida, Yoshio, and Ozki, Shunro, "Sintering of High-Purity Nickel Oxide, II", Journal of the Am. Ceramic Soc., Vol. 42, No. 5, pp 219-228.
4. Jaffe, B., Roth, R.S., and Marzalle, S., "Properties of piezoelectric Ceramics in the Solid Solution Series Lead-Titanate-Lead Zirconate-Lead Oxide", Journal of Research, National Bureau of Standards, 55, (5), November 1955, pp 239-254.
5. Jaffe, Hans, "Piezoelectric Ceramics", Journal of the Am. Ceramic Soc., Vol. 41, p. 494.
6. Kulcsar, Frank, "Electromechanical Properties of Lead-Titanate-Zirconate Ceramics Modified With Certain Three or Five-valent Additions", Journal of the Am. Ceramic Soc., Vol. 42, July 1959.
7. Kulcsar, Frank, "Electromechanical Properties of Lead-Titanate-Zirconate Ceramics With Lead Partially Replaced by Calcium or Strontium", Journal of the Am. Ceramic Soc., Vol. 42, pp 49-51.
8. Nelson, Karl E., and Cook, Ralph L., "Effect of Contamination Introduced During Wet Milling on the Electrical Properties of Barium Titanate", Bulletin of the Am. Ceramic Soc., Vol. 38, No. 10, 1959.
9. Okazaki, Kiyoshi, "High Dielectric Constants Ceramics Containing PbO Especially for the Evaporation of PbO at High Temperatures", Department of Engineering Defense Academy, (11), 1958, p. 74.
10. Quirk, J.F., Mosley, N.B., and Duckworth, W.H., "Characterization of Sinterable Oxide Powders: I, BeO ", Journal of the Am. Ceramic Soc., Vol. 40, (12), 1957, pp 416-419.
11. Quirk, John F., "Factors Affecting Sinterability of Oxide Powders: BeO and MgO ", Journal of the Am. Ceramic Soc., Vol. 42, p. 178.
12. Rosenthal, J.J., and Stoddard, S.D., "A Study of Process Variables in Barium Titanate Ceramics", Bulletin of the Am. Ceramic Soc., Vol. 37, No. 8, 1958.
13. Shirane, Gen., and Suzuki, Kazuo, "Crystal Structure of $Pb(Zr-Ti)O_3$ ", Journal of Physical Society of Japan, 7(3), 333, 1952.